J. Fluid Mech. (1974), *vol.* 62, *part* 1, *pp.* 163–183
Printed in Great Britain

Distorted gas bubbles at large Reynolds number

By M. EL SAWI
Department of Mathematics, Imperial College, London†

(Received 4 December 1972 and in revised form 15 May 1973)

The distortion of a gas bubble rising steadily in an inviscid incompressible liquid of infinite extent under the action of surface tension forces is investigated theoretically using an appropriate extension of the tensor virial theorem. A convenient parameter for distinguishing the bubble shape is the Weber number W. The virial method leads to an expression relating W and the axis ratio χ, of the transverse and longitudinal axes of the bubble. To first order in W, this relation agrees with the linear theory established by Moore (1959). Also, comparison of the results with his (1965) approximate theory reveals similar features and excellent agreement up to $\chi = 2$. In particular, it confirms his prediction of the existence of a maximum Weber number. Although the present work does not consider the stability of these bubbles, it is interesting to note that the maximum value of 3·271 attained by W differs only by about 2·8 % from the critical Weber number obtained by Hartunian & Sears (1957) for the onset of instability.

An approximate method for the study of slightly distorted spheroidal gas bubbles is also formulated and the resulting boundary-value problem solved numerically. The theory is then extended to include gravity. The joint effect of surface tension as well as gravitational forces has not been included in earlier theories. The shapes of the bubbles are traced and compared with the unperturbed spheroids. Comparisons for the velocity of bubble rise are made between the present predictions and some experimental results. In particular the results are compared with recent experimental data for the motion of gas bubbles in liquid metals.

1. Introduction

The virial method has been extended to many different kinds of problem and is widely used in astrophysics. However, its usefulness in hydrodynamic problems has only recently been exploited. A general survey of some of its applications may be found in Chandrasekhar's (1969) book. A recent study of the equilibrium and stability of an incompressible dielectric fluid drop situated in a uniform electric field (Rosenkilde 1969) provides a nice illustration of the method.

It is the purpose of this work to extend the tensor virial theorem of second order for a systematic investigation of the equilibrium of a gas bubble in uniform translational motion with velocity U, through an inviscid incompressible liquid

† Present address: Department of Mathematics, University of Khartoum, Sudan.

of infinite extent, under the action of surface tension. It is assumed that the liquid contains no surfactants, that thermally induced surface tension gradients are negligible (see Harper, Moore & Pearson 1967), that the volume V_b of the bubble is invariant and that the motion of the enclosed gas has a negligible effect on the flow.

It is customary to use as a length scale the 'equivalent spherical radius' r_e, defined by

$$\tfrac{4}{3}\pi r_e^3 = V_b. \tag{1.1}$$

The dimensionless parameters which are of direct dynamical significance are the Reynolds number R and the Weber number W, defined by

$$R = 2r_e \rho U/\mu, \quad W = 2r_e \rho U^2/\sigma \tag{1.2), (1.3}$$

respectively. Here ρ is the density of the surrounding liquid, μ its viscosity, and σ is the interfacial tension. R is taken large enough for boundary-layer ideas to be applicable. It is clear that the surface of the bubble must be stress free, so that the tangential viscous stress component must be continuous across it. As this condition is not satisfied by the ideal flow, a thin boundary layer forms at the bubble surface. Moore (1965) discussed the structure of the boundary layer on an ellipsoidal gas bubble. It was shown that viscous forces in the wake produced no significant modification to the velocity profile of the irrotational flow. Winnikow & Chao (1966) demonstrated the thinness of the wake in the case of droplet motion. In the present work we shall assume that the boundary layer does not separate from the bubble surface, and thus use the irrotational flow field around an oblate spheroid of revolution. The virial analysis for an oblate spheroidal bubble leads to an approximate expression relating W and χ.

To examine larger distortions, we take as our starting point the oblate spheroid, because even for Weber numbers of order unity the bubble might be expected to resemble an oblate spheroid having the same axis ratio. The approximate theory leads to a differential equation for the shape which is then solved numerically.

The method is then extended to examine the effect of gravity as well as surface tension on the shape of the bubble. The formulation of the problem is similar but the Froude number F_r, defined by

$$F_r = U^2/2r_e g^*, \tag{1.4}$$

where g^* is the acceleration due to gravity, enters as a parameter. In actual fact F_r is an unknown parameter in the problem, but this difficulty is resolved by expressing F_r in terms of the drag on the spheroid, which is a known quantity. However this means that the viscosity of the fluid is now a parameter and the equations are solved for different values of M, defined by

$$M = g^*\mu^4/\rho\sigma^3. \tag{1.5}$$

The shapes of the bubbles are traced and compared with the unperturbed spheroids. They are found to be characterized by an indentation at the rear stagnation point.

Finally, the predicted velocity of rise of a gas bubble is tested with some experimental data. Three diverse cases are examined. The rise of air bubbles in water ($M = 2{\cdot}4 \times 10^{-11}$) has often produced discrepancies in experimental results. This is attributed to the fact that water, however pure, is known to contain a small quantity of an unknown surface-active contaminant. The present data are taken from the results of Haberman & Morton (1953). Other data taken from this paper relate to the rise of air bubbles in methyl alcohol ($M = 8{\cdot}9 \times 10^{-11}$). This provides a chance of comparing the present theory with Moore's (1965) earlier theoretical predictions, as well as with known experiments. The theory is also compared with the experimental results for the rise of argon bubbles in mercury ($M = 3{\cdot}7 \times 10^{-14}$; Schwerdtfeger 1968).

2. The appropriate form of the tensor virial theorem

Let S be the surface of the bubble and Σ the surface of a fixed sphere with centre C and a large radius r. Take $\mathbf{n}$ and $\mathbf{N}$ to be unit vectors normal to the surface elements δS and $\delta\Sigma$ and both drawn in the outward directions relative to the closed surfaces S and Σ. The region enclosed between S and Σ is of volume V and is wholly occupied by the liquid. It is convenient to employ a system of rectangular Cartesian co-ordinates $OX_1X_2X_3$ which is moving with the bubble. Its origin† O coincides with the centre of the bubble and has velocity U_i. Also the axis OX_3 is taken parallel to the velocity of the bubble, so that

$$U_1 = U_2 = 0, \quad U_3 = U. \tag{2.1}$$

Let $u_i(x_1, x_2, x_3, t)$ be the liquid velocity relative to Σ. The combination of a moving frame $OX_1X_2X_3$ and a velocity field u_i relative to a fixed frame is slightly unusual, but has advantages for the present problem. One remarks that since Σ is at a large distance and since u_i falls off rapidly with distance from the bubble, u_i does not depend on t; it would, of course, if Σ were at a finite distance. Thus we can obtain the momentum equation in the form

$$\rho u_k \frac{\partial u_i}{\partial x_k} - \rho U_k \frac{\partial u_i}{\partial x_k} = -\frac{\partial P}{\partial x_i}, \tag{2.2}$$

where P is the pressure in the flow field. The advantage of this formulation is that certain integrals over Σ vanish on account of the smallness of u_i. The equation of continuity is

$$\partial u_i / \partial x_i = 0. \tag{2.3}$$

Unless otherwise stated, the summation convention applies to repeated indices in the above equations only.

Now to obtain the second-order virial equation, we have simply to multiply (2.2) by x_j and integrate over the entire volume V occupied by the liquid. Thus the first moment of the equation of motion is

$$\int_V \rho x_j u_k \frac{\partial u_i}{\partial x_k} dV - \int_V \rho x_j U_k \frac{\partial u_i}{\partial x_k} dV = -\int_V x_j \frac{\partial P}{\partial x_i} dV, \tag{2.4}$$

where

$$dV = dx_1\, dx_2\, dx_3 \tag{2.5}$$

† At time $t = 0$, O and C are taken coincident.

is the volume element. Applying the divergence theorem to the right-hand side of (2.4) gives

$$-\int_V x_j \frac{\partial P}{\partial x_i}\, dV = \int_S x_j P\, dS_i + 2R_{ij} + \Pi\delta_{ij}, \tag{2.6}$$

where δ_{ij} is the Kronecker delta and

$$dS_i = n_i\, dS, \quad d\Sigma_i = N_i\, d\Sigma, \tag{2.7}$$

where n_i and N_i denote the components of $\mathbf{n}$ and $\mathbf{N}$ respectively. The tensor

$$R_{ij} = -\frac{1}{2}\int_\Sigma x_j P\, d\Sigma_i \tag{2.8}$$

represents the effect of the disturbance on the pressure at the surface Σ and, in general, it is non-zero even when Σ recedes to infinity. Finally, the scalar quantity

$$\Pi = \int_V P\, dV \tag{2.9}$$

accounts for the microscopic motion of the liquid particles.

Now the external pressure on S is given by Laplace's formula

$$P_{nn} - P_g = -\sigma \nabla . \mathbf{n}, \tag{2.10}$$

where P_{nn} is the normal stress and is equal to the pressure P in the irrotational flow plus the viscous normal stress, which is smaller by a factor $O(R^{-1})$ and whose contribution is therefore neglected. P_g is the gas pressure inside the bubble and is an unknown constant. Thus (2.10) reduces to

$$P - P_g = -\sigma \nabla . \mathbf{n}. \tag{2.11}$$

Using this boundary condition, the integral on the right-hand side of (2.6) may be rewritten in the form

$$\int_S x_i P\, dS_i = -2C_{ij} + K_{ij}, \tag{2.12}$$

where

$$C_{ij} = \frac{\sigma}{2}\int_S x_j \nabla . \mathbf{n}\, dS_i \tag{2.13}$$

is the surface-energy tensor, see Rosenkilde (1967). The tensor

$$K_{ij} = P_g \int_S x_j\, dS_i \tag{2.14}$$

will be identified as the gas tensor. The next task is to transform the left-hand side of (2.4) into simpler integrals. After simple manipulations and application of the divergence theorem, the first integral gives

$$\int_V \rho x_j u_k \frac{\partial u_i}{\partial x_k}\, dV = -\int_V \rho u_i u_j\, dV + 2L_{ij} + 2L'_{ij}, \tag{2.15}$$

where

$$L_{ij} = -\frac{1}{2}\int_S \rho x_j u_i u_k\, dS_k, \quad L'_{ij} = \frac{1}{2}\int_\Sigma \rho x_j u_i u_k\, d\Sigma_k. \tag{2.16), (2.17}$$

We can perform some further useful transformations once we have introduced the assumption of irrotational flow

$$u_i = \partial\Phi_i/\partial x_i, \tag{2.18}$$

where Φ is the velocity potential. On substituting this value of u_i in the integral on the right-hand side of (2.15) and applying the divergence theorem, we get

$$\int_V \rho u_i u_j \, dV = 2T_{ij} + 2T'_{ij} + 2N_{ij}, \tag{2.19}$$

where

$$T_{ij} = -\frac{1}{2}\int_S \rho\Phi u_j \, dS_i, \quad T'_{ij} = \frac{1}{2}\int_\Sigma \rho\Phi u_j \, d\Sigma_i \tag{2.20), (2.21}$$

and

$$N_{ij} = -\frac{1}{2}\int_V \rho\Phi \frac{\partial u_j}{\partial x_i} \, dV. \tag{2.22}$$

Here T_{ij} is the kinetic-energy tensor and the contraction of it gives

$$T = -\frac{1}{2}\int_S \rho\Phi \frac{\partial\Phi}{\partial n} \, dS. \tag{2.23}$$

where T is the kinetic energy associated with the macroscopic motion of the liquid.

By similar calculations, the second integral on the left-hand side of (2.4) becomes

$$\int_V \rho x_j U_k \frac{\partial u_i}{\partial x_k} \, dV = 2(M_{ij} + M'_{ij} + Q_{ij} + Q'_{ij}), \tag{2.24}$$

where

$$M_{ij} = -\frac{1}{2}\int_S \rho u_i x_j U_k \, dS_k, \quad M'_{ij} = \frac{1}{2}\int_\Sigma \rho u_i x_j U_k \, d\Sigma_k, \tag{2.25), (2.26}$$

$$Q_{ij} = \frac{1}{2}\int_S \rho\Phi U_j \, dS_i, \quad Q'_{ij} = -\frac{1}{2}\int_\Sigma \rho\Phi U_j \, d\Sigma_i. \tag{2.27), (2.28}$$

Finally, on substituting from (2.6)–(2.28) into (2.4) one gets

$$L_{ij} + L'_{ij} = T_{ij} + T'_{ij} + N_{ij} + R_{ij} + M_{ij} + M'_{ij} + Q_{ij} + Q'_{ij} - C_{ij} + \tfrac{1}{2}K_{ij} + \tfrac{1}{2}\Pi\delta_{ij}, \tag{2.29}$$

which is the tensor virial equation of second order. It provides a set of nine moment equations since

$$i, j = \{1, 2, 3\}. \tag{2.30}$$

3. The method of solution

The application of the virial method requires the selection of a trial shape. Though the equations of equilibrium cannot be completely satisfied over the surface of an oblate spheroid in a uniform flow field unless the Weber number is small, to be consistent with experimental evidence and previous theoretical models (Siemes 1954; Saffman 1956; Hartunian & Sears 1957; Moore 1965) the bubble shape will be explicitly assumed to take the form

$$\frac{x_1^2 + x_2^2}{a_1^2} + \frac{x_3^2}{a_3^2} = 1, \tag{3.1}$$

where $a_1 > a_3$. This is an oblate spheroid whose axis of symmetry OX_3 is parallel to the velocity of the bubble. As a trial shape, it has the advantage that relatively simple expressions for the velocity field are available, e.g. in Lamb (1959).

In order to evaluate the various tensorial quantities appearing in the virial equation, one requires the system of oblate spheroidal co-ordinates. This system is related to rectangular Cartesian co-ordinates by the equations

$$x_1 = \varpi \cos\gamma, \quad x_2 = \varpi \sin\gamma, \quad x_3 = z = k\alpha\beta, \tag{3.2}$$

where

$$\varpi = k[(1+\alpha^2)(1-\beta^2)]^{\frac{1}{2}}. \tag{3.3}$$

The surfaces $\alpha = \alpha_0$ (= constant) are oblate spheroids of revolution about OX_3 and are given by (3.1), thus leading to the relations

$$a_1 = k(1+\alpha_0^2)^{\frac{1}{2}}, \quad a_3 = k\alpha_0. \tag{3.4}$$

The line elements h_α, h_β and h_γ defined by

$$dS^2 = h_\alpha^2 d\alpha^2 + h_\beta^2 d\beta^2 + h_\gamma^2 d\gamma^2 \tag{3.5}$$

are given by

$$h_\alpha = k(D/L)^{\frac{1}{2}}, \quad h_\beta = k(D/E)^{\frac{1}{2}}, \quad h_\gamma = k(LE)^{\frac{1}{2}}, \tag{3.6}$$

where the notation

$$\left.\begin{aligned} D &= \alpha^2+\beta^2, \quad L = 1+\alpha^2, \quad E = 1-\beta^2, \\ D_0 &= \alpha_0^2+\beta^2, \quad L_0 = 1+\alpha_0^2 \end{aligned}\right\} \tag{3.7}$$

is now introduced.

The motion due to an oblate spheroid $\alpha = \alpha_0$ relative to a fixed frame moving with velocity U parallel to its axis of revolution in an infinite mass of liquid, as given in Lamb (1959, p. 144), is

$$\Phi = c_0\beta(\alpha \cot^{-1}\alpha - 1), \tag{3.8}$$

where

$$c_0 = kU/(\cot^{-1}\alpha_0 - \alpha_0/L_0). \tag{3.9}$$

The velocity components along the Cartesian axes are found to be

$$u_1 = c_0\beta x_1/k^2LD, \quad u_2 = c_0\beta x_2/k^2LD, \quad u_3 = c_0(D\cot^{-1}\alpha)/kD. \tag{3.10}$$

The above relations are used to evaluate the different quantities in the tensor virial equation (2.29). Although the computations are straightforward, they are lengthy and tedious. The actual calculations and values of the tensors may be found in El Sawi (1970). In particular, it is found that all the tensors are diagonal, and that L'_{ij} and T'_{ij} are identically zero. Accordingly, (2.29) reduces to

$$L_{ii} = T_{ii} + N_{ii} + R_{ii} + M_{ii} + M'_{ii} + Q_{ii} + Q'_{ii} - C_{ii} + \tfrac{1}{2}(P_g V_b + \Pi). \tag{3.11}$$

This provides a set of three equations ($i = 1, 2, 3$). Two of these equations ($i = 1, 2$) are identical because of symmetry about OX_3.

Now, upon eliminating the constant $P_g V_b + \Pi$ from (3.11) and substituting for each element its value in terms of χ, one obtains

$$W = \frac{2(h\chi^2-g)^2[g\chi(3\chi^2-g^2) - (3\chi^2+g^2)\tanh^{-1}(g/\chi)]}{g^4(3h\chi^2 - 2hg^2 - 3g)\chi^{\frac{7}{3}}}, \tag{3.12}$$

where

$$g = (\chi^2-1)^{\frac{1}{2}}, \quad h = \sec^{-1}\chi. \tag{3.13}$$

This expression for W constitutes the main result of this paper. Another useful result is the expression for the gas pressure P_g, which may be obtained from the contracted form of the virial equation (3.11). The trace of this equation is

$$L = T+N+R+M+M'+Q+Q'-C+\tfrac{3}{2}(P_g V_b+\Pi), \tag{3.14}$$

where C is the surface energy. Equation (3.14) represents the scalar form of the virial theorem appropriate for a gaseous bubble rising in an infinite liquid. On substituting for the different quantities in this equation, one obtains the expression

$$P_g = \frac{2[g\chi+\tanh^{-1}(g/\chi)]}{gW\chi^{\frac{1}{2}}}+\frac{3h\chi^3+2g^3(1-\chi)-3g\chi^3}{6(h\chi^3-g\chi)} \tag{3.15}$$

for the dimensionless gas pressure P_g.

4. Nearly spheroidal gas bubbles

An approximate theory, based on the above virial result (3.12), is developed here for the study of nearly spheroidal bubbles. The same physical assumptions are made in the present case. The effect of surface tension on the deformation of spheroidal bubbles is considered first. Then the theory is extended to examine the joint effect of surface tension and gravitational forces.

The problem is to determine a surface S on which the boundary condition (2.11) is satisfied. This condition may be written in the alternative form

$$P+\sigma J = P_g, \tag{4.1}$$

where

$$J = 1/R_1+1/R_2 \tag{4.2}$$

is the first curvature of S, and R_1 and R_2 are the principal radii of curvature. The pressure P is determined from Bernoulli's equation

$$P+\tfrac{1}{2}\rho(u_n^2+u_t^2) = P_s, \tag{4.3}$$

where P_s is the stagnation pressure and u_n and u_t are the normal and tangential components of the velocity, bearing in mind that u_n vanishes on the bubble surface. The bubble shape S is represented in oblate spheroidal co-ordinates by the surface of revolution

$$G = \alpha-\alpha_0-g(\beta) = 0, \tag{4.4}$$

where $\alpha = \alpha_0$ is the spheroid which has the same volume as the exact shape and is closest to it in some sense. We shall call this the basic spheroid. In the subsequent approximate theory, α_0 is determined by the virial result (3.12).

Thus we seek a gas pressure P_g, a constant α_0 and a continuous function $g(\beta)$ such that

$$P_s-\tfrac{1}{2}\rho u_t^2+\sigma J = P_g, \tag{4.5a}$$

$$\text{volume of } G = V_b, \tag{4.5b}$$

where in (4.5a) u_t is the slip velocity and J is the first curvature for the surface (4.4). The derivation of J, in orthogonal curvilinear co-ordinates, is described in the appendix. By straightforward calculations and substitution into equation

(A 5) in the appendix, the expression for J corresponding to the surface (4.4) is found to be

$$J = kH/[D(L+Eg^2)]^{\frac{3}{2}}, \tag{4.6}$$

where

$$H = L(2L-E)\alpha + L(2L-3E)\beta g - ELD\ddot{g} + (3L-2E)\alpha Eg^2 + E(L-2E)\beta g^3, \tag{4.7}$$

using the notation of (3.7). The size of the bubble enters the above equations through k and it will be convenient to remove this dependence by introducing r_e. Since the basic spheroid is chosen to have the same volume as the true shape, on making use of (1.1), one gets

$$r_e = k(\alpha_0 L_0)^{\frac{1}{3}}. \tag{4.8}$$

The above boundary condition (4.5a) may be written in the form

$$2\delta P + 4J(\alpha_0 L_0)^{\frac{1}{3}}/W = u_t^2, \tag{4.9}$$

where

$$\delta P = P_s - P_g. \tag{4.10}$$

The expression (4.6) for the first curvature is now

$$J = H/[D(L+E\dot{g}^2)]^{\frac{3}{2}}. \tag{4.11}$$

Consider now the surface (4.4), for small g, such that

$$\alpha = \alpha_0 + g(\beta) + O(g^2). \tag{4.12}$$

Substituting this in (4.11) leads to

$$J = J_0 + \bar{J} + O(g^2), \tag{4.13}$$

where

$$J_0 = (2L_0 - E)\alpha_0/L_0^{\frac{1}{2}}D_0^{\frac{3}{2}} \tag{4.14}$$

is the first curvature for the spheroid α_0 and

$$\bar{J} = L_0^{-\frac{3}{2}}D_0^{-\frac{5}{2}}[L_0 D_0(2L_0 - 3E)\beta\dot{g} - L_0 D_0^2 E\ddot{g} + (-2L_0^3 + 4L_0^2 - L_0^2 E - 2L_0 E + E^2)g] + O(g^2). \tag{4.15}$$

Similarly the slip velocity u_t corresponding to the surface (4.12) may be written in the form

$$u_t = u_\beta^{(0)} + u_\beta^{(1)} + \ldots, \tag{4.16}$$

where $u_\beta^{(0)}$ is the slip velocity on the spheroidal surface α_0 and is readily calculated in the form

$$u_\beta^{(0)} = Uc_1 E^{\frac{1}{2}} L_0^{-1} D^{-\frac{1}{2}}, \tag{4.17}$$

where

$$c_1 = 1/(\cot^{-1}\alpha_0 - \alpha_0/L_0). \tag{4.18}$$

The second term $u_\beta^{(1)}$ represents the velocity perturbation.

Upon substituting from (4.13) and (4.16) into the equilibrium condition (4.9) one finds that

$$(\alpha_0 L_0)^{\frac{1}{3}}(J_0 + \bar{J}) - \tfrac{1}{4}W(u_\beta^{(0)2} + \lambda) = -\tfrac{1}{2}W\delta P + O(g^2), \tag{4.19}$$

where

$$\lambda = u_\beta^{(1)2} + 2u_\beta^{(0)}u_\beta^{(1)} + \ldots \tag{4.20}$$

is the velocity perturbation term. It is always possible to choose W small enough so that the condition

$$\lambda W = O(g^2) \tag{4.21}$$

may be satisfied. Moore (1959) has shown that the velocity corrections lag one step, in the perturbation scheme, behind the shape corrections. In the present theory we shall assume that condition (4.21) is satisfied for all W, so that (4.19) reduces to

$$(\alpha_0 L_0)^{\frac{1}{3}}(J_0+\bar{J})-\tfrac{1}{4}Wu_\beta^{(0)2}=-\tfrac{1}{2}W\delta P+O(g^2). \tag{4.22}$$

This is the basis of the approximate method which we shall introduce in the next section.

5. Linearized virial theory

Having introduced the approximate method based on the hypothesis that the true shape of the bubble will differ little from the basic spheroid, we can use the flow field about this spheroid to determine the dynamic pressure on the surface of the true shape. Then the equilibrium condition (4.22) becomes a differential equation for g, and this is solved numerically.

Upon substituting from (4.15) into (4.22) one gets

$$A(\beta,\chi)\ddot{g}+B(\beta,\chi)\dot{g}+C(\beta,\chi)g=F(\beta,\chi)+a(\chi)+O(g^2), \tag{5.1}$$

which is a linear second-order inhomogeneous differential equation in g. The function $F(\beta,\chi)$ is given by

$$F(\beta,\chi)=\tfrac{1}{4}Wu_\beta^{(0)2}-J_0(\alpha_0 L_0)^{\frac{1}{3}}, \tag{5.2}$$

and $a(\chi)$ is a constant which varies with the axis ratio. The coefficients A, B and C in (5.1) are given by

$$\left.\begin{aligned}
A(\beta,\chi)&=-E(\alpha_0 L_0)^{\frac{1}{3}}(D_0 L_0)^{-\frac{1}{2}},\\
B(\beta,\chi)&=\beta(2L_0-3E)(\alpha_0 L_0)^{\frac{1}{3}}D_0^{-\frac{3}{2}}L_0^{-\frac{1}{2}},\\
C(\beta,\chi)&=(-2L_0^3+4L_0^2-L_0^2E-2L_0E+E^2)(\alpha_0 L_0)^{\frac{1}{3}}D_0^{-\frac{5}{2}}L_0^{-\frac{3}{2}}.
\end{aligned}\right\} \tag{5.3}$$

In particular,

$$A(\pm 1,\chi)=B(0,\chi)=0. \tag{5.4}$$

Thus for any given value $\chi=\chi_0$, the functions A, B, C and F in equation (5.1) are all known, and the corresponding value for W in (5.2) is obtained on substituting for χ_0 into (3.12). However, the unknown constant $a(\chi)$ has still to be determined. It is also clear from (5.4) that (5.1) has a regular singularity at $\beta=\pm 1$.

It is evident that (5.1) requires three conditions to determine the general solution. To accomplish this let us use the assumption that the bubble has fore-and-aft symmetry. This implies, using (3.2) and (3.3), that the co-ordinate axes OZ and $O\varpi$, in a meridian section of the bubble, are normals to the trace of the bubble. In other words,

$$[d\varpi/dz]_{\beta=0}=0, \quad [dz/d\varpi]_{\beta=1}=0. \tag{5.5), (5.6}$$

Performing the differentiation in (5.5), on the understanding that $\alpha>0$ for all β, the condition is found to be equivalent to

$$\dot{g}(\beta)=0 \quad \text{at} \quad \beta=0. \tag{5.7}$$

The latter condition (5.6), for the slope to be zero at the pole, is satisfied by any regular solution of the differential equation (5.1). Therefore we shall impose regularity of the solution at the pole. This leads to, from (5.1),

$$B(1,\chi)\dot{g}(1)+C(1,\chi)g(1)-F(1,\chi)=a(\chi). \tag{5.8}$$

A third condition is necessary to determine the unknown constant $a(\chi)$ in (5.1). Now as the volume of the bubble is to be prescribed, we normalize its value to that of the spheroid α_0. This is equivalent to the relation

$$\int_0^1 g(\beta)\,D_0\,d\beta = 0.$$

The conditions on (5.1) can now be summarized as follows:

$$\dot{g}(\beta)=0 \quad \text{at} \quad \beta=0, \tag{5.9a}$$

$$B(1,\chi)\dot{g}(1)+C(1,\chi)g(1)-F(1,\chi)=a(\chi), \tag{5.9b}$$

$$\int_0^1 g(\beta)\,D_0\,d\beta = 0. \tag{5.9c}$$

We now embark on solving the problem numerically using the method described by Fox (1957, chap. 8). The basic process is to solve the boundary-value problem using an initial-value technique. One starts by solving the problem with some arbitrary initial conditions, combining the solutions to satisfy all the given boundary conditions.

Consider now the inhomogeneous equation (5.1) together with the corresponding homogeneous equation

$$A(\beta,\chi)\ddot{g}+B(\beta,\chi)\dot{g}+C(\beta,\chi)g=0. \tag{5.10}$$

Equation (5.1) can now be integrated completely with the two-point boundary conditions (5.9a) and (5.9b). The numerical procedure is as follows.

(i) Guess a value for $a(\chi)$.

(ii) Define $g_{\mathrm{I}}(\beta)$ to satisfy (5.1) and such that at $\beta=1$

$$\left.\begin{aligned} B(1,\chi)\dot{g}_{\mathrm{I}}(1)+C(1,\chi)g_{\mathrm{I}}(1)&=a(\chi),\\ g_{\mathrm{I}}(1)&=1. \end{aligned}\right\} \tag{5.11}$$

(iii) Define $g_{\mathrm{II}}(\beta)$ to satisfy (5.10) and such that at $\beta=1$

$$\left.\begin{aligned} B(1,\chi)\dot{g}_{\mathrm{II}}(1)+C(1,\chi)g_{\mathrm{II}}(1)&=0,\\ g_{\mathrm{II}}(1)&=1. \end{aligned}\right\} \tag{5.12}$$

Clearly

$$g(\beta)=g_{\mathrm{I}}(\beta)+tg_{\mathrm{II}}(\beta) \tag{5.13}$$

satisfies (5.1) and boundary condition (5.9b). Now choose t such that $g(\beta)$ satisfies boundary condition (5.9a). This yields

$$t=-\dot{g}_{\mathrm{I}}(0)/\dot{g}_{\mathrm{II}}(0). \tag{5.14}$$

(iv) Choose $a(\chi)$ such that (5.9c) is satisfied. This can be achieved using the following iterative procedure.

The integral in (5.9*c*) is denoted by y, where y is then a function of $a(\chi)$, and so one has to find a value for a such that y vanishes. Suppose that $a+\delta a$ is the exact value for which y is zero. Then, using Taylor's theorem, one gets

$$y(a+\delta a) = y(a)+\delta a\, dy/da+\ldots = 0.$$

Therefore
$$\delta a = -y(a)/(dy/da). \tag{5.15}$$

Now to calculate dy/da let the initial δa be δa_0. Then

$$\frac{dy}{da} = \frac{y(a+\delta a_0)-y(a)}{\delta a_0}.$$

Hence by (5.15) one finds

$$\delta a_1 = -\frac{y(a)\,\delta a_0}{y(a+\delta a_0)-y(a)},$$

where δa_1 is the new value for δa. Thus the general equation used to correct a is

$$\delta a_{n+1} = -\frac{y(a_n)\,\delta a_n}{y(a_n+\delta a_n)-y(a_n)}, \tag{5.16}$$

where
$$a_{n+1} = a_n+\delta a_n \tag{5.17}$$

and a_n is the nth approximation to a.

The numerical integration of (5.1) is carried out using the fourth-order Runge–Kutta method with step width

$$\delta\beta = 0{\cdot}002. \tag{5.18}$$

Upon reducing $\delta\beta$ to 0·0002, no significant change was detected in the results. It seems therefore that there is no appreciable build up of error resulting from reducing the step width to this value.

The solution is started with a prescribed value $\chi = \chi_0$, say. This fixes the values of α_0 and W. Also the coefficients A, B and C together with J_0 and $u_\beta^{(0)}$ are computed, at the specified number of points on the bubble surface, using this value of χ.

In order to start the integration of (5.1), the value of $a(\chi)$ is required. However, this is not known in advance, in consequence it has to be determined by a trial-and-error solution. A value is guessed for it and the integration is then started from the pole and towards the equator (i.e. along the direction of the flow). In order to force the regularity of the solution at $\beta = 1$, the integration is started a few steps away from $\beta = 1$, precisely at $\beta = 0{\cdot}996$. This is accomplished by finding the series solution of (5.1) in the neighbourhood of $\beta = 1$ and selecting a few terms of the power series of the regular solution. This, however, has been found to have no advantages, in this problem, over the case when the integration is started exactly at $\beta = 1$. Both results are found to be identical, to the required degree of accuracy. This result is, otherwise, expected from the fact that the singularity in (5.1) at $\beta = 1$ is regular.

In the iteration process it has been found that, to avoid running into a loop of oscillating convergence, it is necessary to add a fraction of δa_n at a time instead of the whole increment as in (5.17). The relation that has been employed instead is

$$a_{n+1} = a_n+\tfrac{2}{5}\delta a_n. \tag{5.19}$$

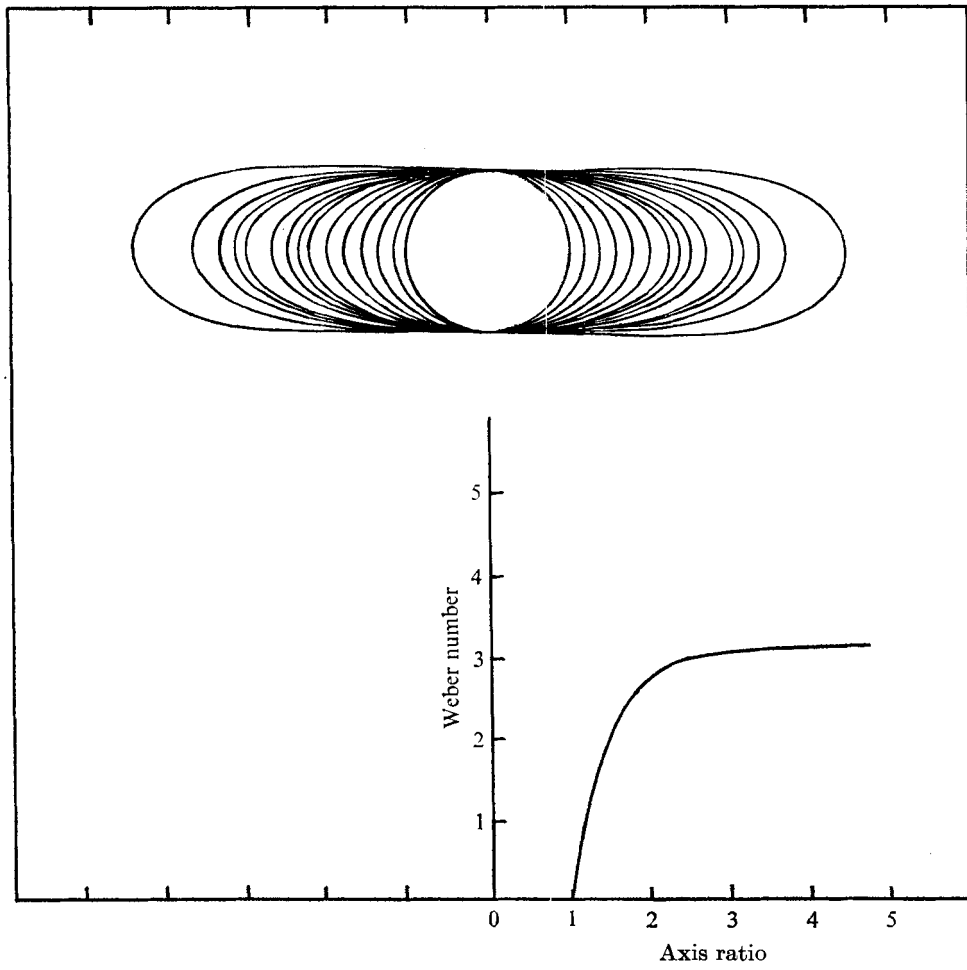

FIGURE 1. Variation of the Weber number with the axis ratio for a family of symmetric bubbles obtained by linear perturbation of an oblate spheroid. The horizontal scale represents the same axis ratio for both diagrams. The relation between the Weber number and the axis ratio is that given by the 'linearized virial theory'.

This has given rise to an average of about ten iterations necessary to obtain an accuracy of $a(\chi)$ to three decimal places.

The program required about 10 min of computer time. It should be noted here that the iterative procedure was set to stabilize three decimal places. By reducing the tolerances in the iteration process and reducing $\delta\beta$, greater accuracy could have been obtained but of course more machine time would have been involved.

In figure 1 a sequence of bubble shapes is traced for different values of the Weber number. Thus, under the action of surface tension alone, the bubble seems to deform with increasing W from the spherical shape into a spheroidal one and then into a disk-shaped bubble and then probably into a toroidal shape. Whether all these shapes are stable remains to be investigated.

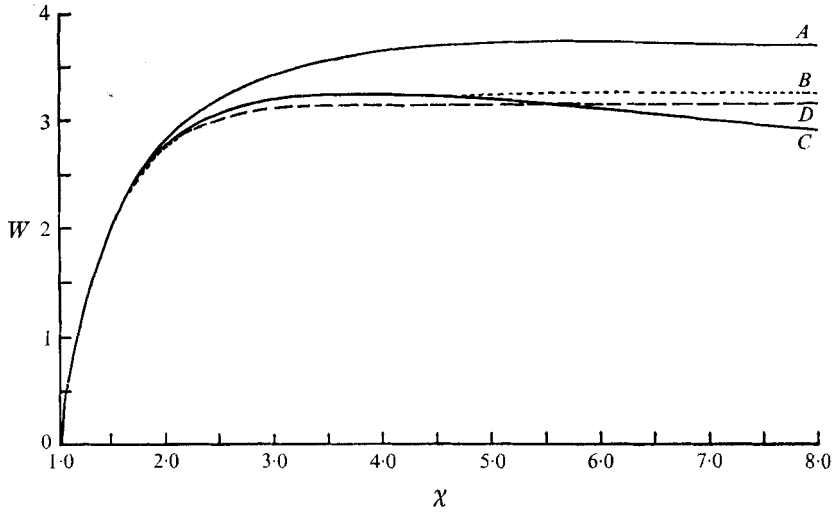

FIGURE 2. Variation of the Weber number with the axis ratio. *A*, two-point theory; *B*, linearized two-point theory; *C*, virial theory; *D*, linearized virial theory.

Moore (1965), using an approximate 'two-point theory', obtained an expression relating the Weber number and the axis ratio. Using this relation instead of that of the virial theory and solving the differential equation (5.1) again, one obtains another relation for the variation of W with χ. This we shall refer to as the 'linearized two-point theory'. In figure 2 comparisons are given for the variation of the Weber number with the axis ratio; the relations corresponding to the virial theory, the 'two-point theory' and the 'linearized two-point theory' are plotted. It is reassuring to note the tendency of the two linearized versions to converge towards each other.

6. The effect of gravity

Hitherto, our investigations have been confined to motions which take no account of gravity. This section is devoted to examining the effect of gravitational forces, in the presence of surface tension, on a rising bubble.

Gravity forces become significant when the hydrostatic pressure is comparable with the hydrodynamic pressure, i.e.

$$\rho g^* r_e \sim \rho U^2.$$

Now in the steady state, the drag force equals the buoyancy force, i.e.

$$\tfrac{1}{2}\rho U^2 \pi r_e C_D = \tfrac{4}{3}\pi r_e^3 \rho g^*,$$

or

$$C_D = 8g^* r_e / 3U^2, \tag{6.1}$$

where C_D is the drag coefficient. It is now apparent that gravity becomes important when C_D is $O(1)$.

Apart from minor modifications, the method is practically the same as that for surface tension alone. In the present case Bernoulli's equation becomes

$$P + \tfrac{1}{2}\rho u_\beta^{(0)2} - \rho g^* z = \text{constant}. \tag{6.2}$$

Now taking the surface of the bubble to be as in (4.12) and assuming that it has the same velocity field as that of the unperturbed spheroid α_0, one gets in dimensionless form the equation

$$A(\beta,\chi)\ddot{g}+B(\beta,\chi)\dot{g}+C(\beta,\chi)g = F(\beta,\chi)-Wz(r_eF_r)^{-1}+\text{constant}. \tag{6.3}$$

This equation is similar to (5.1), the terms having the same meaning. Now for a point on the surface of the bubble

$$z = \alpha\beta = \alpha_0\beta+\beta g(\beta)+O(g^2), \tag{6.4}$$

in dimensionless form. Combining (6.3) and (6.4) one gets on the surface of the bubble

$$A(\beta,\chi)\ddot{g}+B(\beta,\chi)\dot{g}+\bar{C}(\beta,\chi)g = \bar{F}(\beta,\chi)+\bar{a}(\chi), \tag{6.5}$$

where
$$\bar{C} = C(\beta,\chi)+\beta W/F_rr_e, \quad \bar{F}(\beta,\chi) = F(\beta,\chi)-\alpha_0\beta W/F_rr_e, \tag{6.6}$$

with $\bar{a}(\chi)$ playing the same role as $a(\chi)$ in (5.1). It now remains to determine the Froude number. From (1.4) and (6.1) one obtains the relation

$$F_r = 4/3C_D, \tag{6.7}$$

so that one may also assert that, for $F_r = O(1)$, gravity forces come into play.

From the expressions defining the parameters M, R, W and C_D, it is a simple matter to show that

$$C_D = \tfrac{4}{3}MR^4W^{-3}. \tag{6.8}$$

Now availing ourselves of the expression for C_D, obtained by Moore (1965),

$$C_D = (48/R)\,G(\chi)+O(R^{-\frac{3}{2}}), \tag{6.9}$$

where
$$G(\chi) = \frac{\chi^{\frac{4}{3}}(\chi^2-1)^{\frac{3}{2}}[(\chi^2-1)^{\frac{1}{2}}-(2-\chi^2)\sec^{-1}\chi]}{3(\chi^2\sec^{-1}\chi-(\chi^2-1)^{\frac{1}{2}})^2}, \tag{6.10}$$

it will be possible to find F_r and R for any spheroid whose axis ratio is known. This is accomplished by prescribing values for M and χ. It is then possible to determine W and $G(\chi)$. Combining (6.8) and (6.9) one finds

$$R = (36W^3G(\chi)/M)^{\frac{1}{5}}, \tag{6.11}$$

which determines the value of the Reynolds number. It is then a simple matter to determine C_D and F_r.

Having found the necessary parameters, we now proceed to solve (6.5) numerically. The technique used resembles that adopted for the solution of (5.1). One starts with a given spheroid α_0 whose axis ratio is χ_0, and a prescribed value for M. Knowing χ_0 and M, one determines r_e, W, $G(\chi)$, R, C_D, F_r and U. It is important to notice that, in this procedure, the Weber number is the key parameter and once it is specified, the remaining parameters including the bubble shape are determined. Apart from the fact that the numerical integration now runs from the forward stagnation point to the rear stagnation point the other steps and assumptions are all applied as for the symmetric case.

It is a simple matter to calculate the values of W, R, C_D and F_r, corresponding to χ_0, using the relevant expressions. The results indicate a minimum of C_D

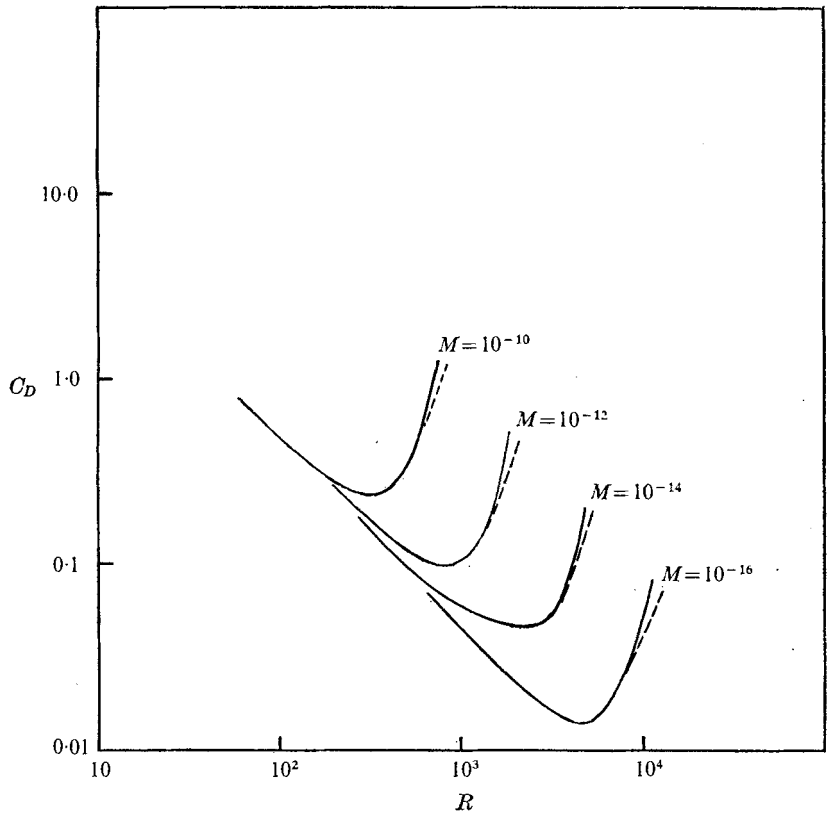

FIGURE 3. The theoretical drag coefficient as a function of the Reynolds number. ——, two-point theory; – – – –, virial theory. The right-hand end of the curves corresponds to an axis ratio $\chi = 6$.

at $W = 1{\cdot}91$, corresponding to $\chi_0 = 1{\cdot}44$. Moore (1965), including the effect of the boundary layer in computing C_D, found that the minimum of C_D occurs at $W = 1{\cdot}8$. Other features predicted by his theory are also observed in the present one. It seems to support his speculation that "the drag coefficient is not very sensitive to the shape of the bubble once the axis ratio is fixed". The present theory predicts the rise of C_D with R (figure 3) after reaching its minimum value but not so sharply as in Moore's theory. This is probably because boundary-layer effects have not been included in the present work.

7. Comparison with experiment

The most extensive experimental results with which we can compare the theoretical predictions are those of Haberman & Morton (1953). Comparisons are also made with recent experimental results of Jones (1965) and Schwerdtfeger (1968). The theory is tested by comparing its predictions of the velocity of rise as a function of r_e. An attempt is also made to compare the shapes of the bubbles. In figures 4 and 5, the shapes predicted by the present theory are traced using

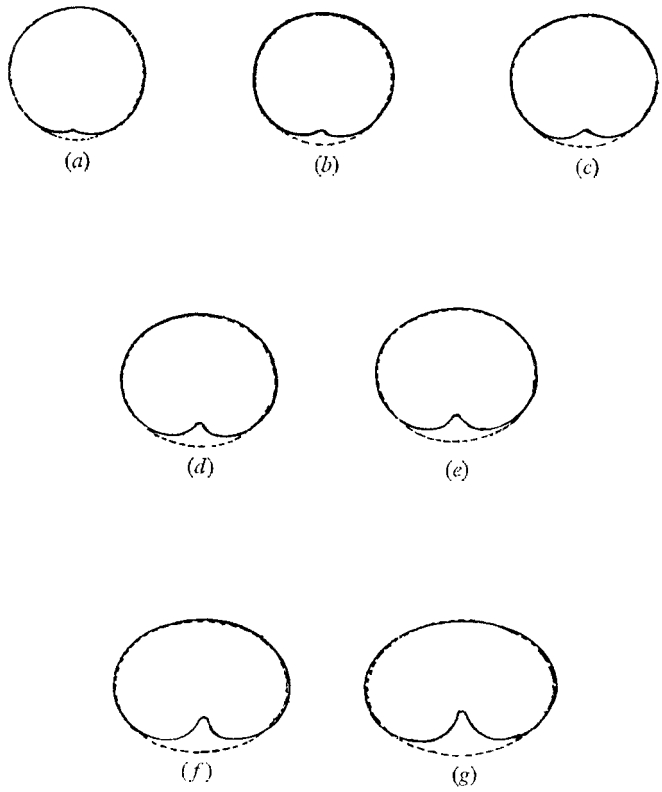

FIGURE 4. Shapes predicted by the virial theory for air bubbles in distilled water ($M = 2{\cdot}4 \times 10^{-11}$). – – –, basic spheroid; ——, theoretical bubble shape.

continuous lines, while those of the spheroids α_0 are shown as broken lines. Plots of U as a function of r_e for air bubbles in methyl alcohol and in water, and for argon bubbles in mercury are shown in figures 6 and 7. Comparison of the theory with experiment for water shows a slightly higher value for U than the corresponding experimental values of Haberman & Morton. Also the maximum value of U occurs at a larger r_e than that given by experiment. Moore (1965) noticed such a discrepancy in comparing his theory for methyl alcohol with Haberman & Morton's experimental curve. The present theory for methyl alcohol reveals similar features. In particular, it is also observed that for $\chi > 2$ reasonable agreement between theory and experiment still exists.

It is interesting to note that the virial theory gives, for all three liquids, a maximum value of U at an axis ratio $\chi_0 = 1{\cdot}9$ with a corresponding value of $W = 2{\cdot}70$. Similar calculations using the 'two-point theory' give $\chi_0 = 1{\cdot}9$ with a corresponding value of $W = 2{\cdot}73$. It seems therefore that, for low M liquids, the axis ratio is a crucial parameter in the sense that, once it is fixed, it is possible to determine the drag coefficient and the velocity of rise irrespective of the bubble shape. It is necessary to make further investigations on this point owing to the fact that the present theory does not account for the presence of a boundary layer on the surface of the bubble.

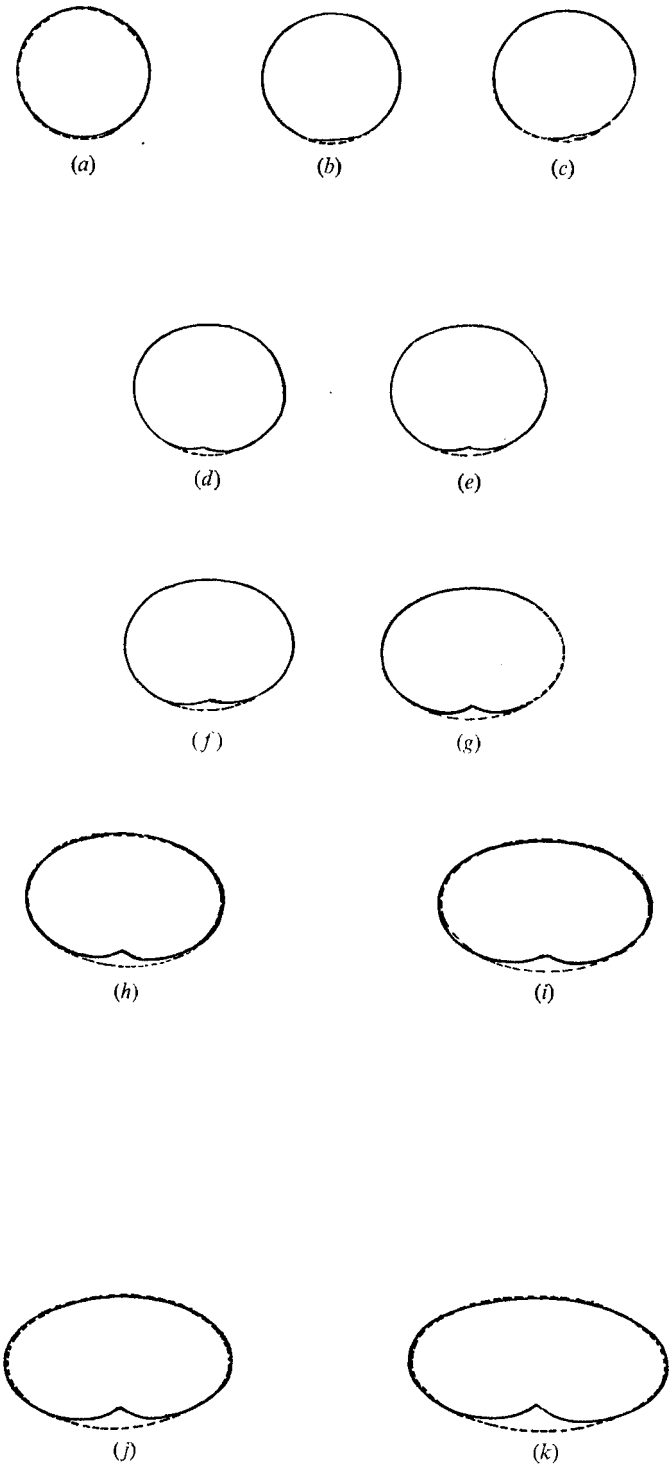

FIGURE 5. Shapes predicted by the virial theory for argon bubbles in mercury ($M = 3{\cdot}7 \times 10^{-14}$). – – –, basic spheroid. ——, theoretical bubble shape.

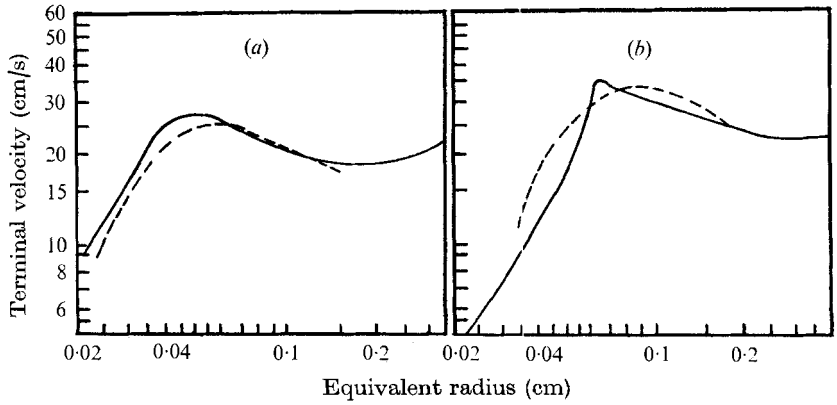

FIGURE 6. Comparison of theory and experiment for air bubbles (*a*) in methyl alcohol and (*b*) in distilled (or filtered) water. – – – –, virial theory; ——, smoothed experimental curve (Haberman & Morton).

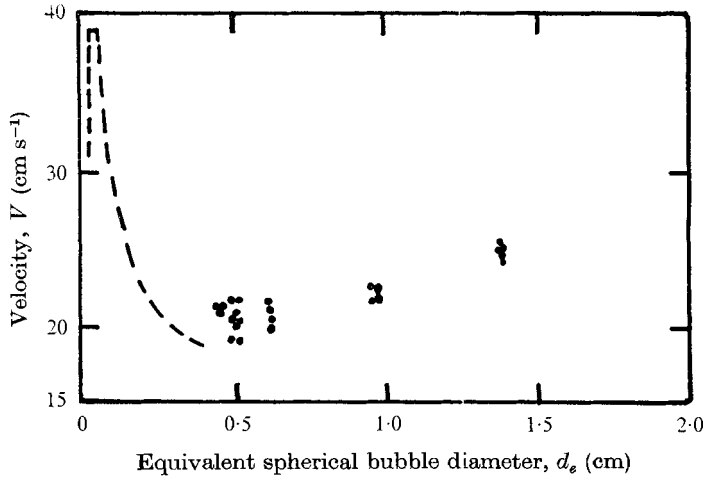

FIGURE 7. Comparison of theory and experiment, – – – –, virial theory; ●, experimental work (Schwerdtfeger).

Comparison of the theory with the experimental results of Schwerdtfeger, for argon bubbles rising in mercury, shows fair agreement. It is disappointing that no results for smaller r_e are available for mercury because the present theory decreases in accuracy as r_e increases.

The size of bubbles dealt with in this work is of the order of a few millimetres. It is therefore not surprising that experimenters find it rather difficult to obtain clearer photographs for such bubbles. Haberman & Morton give photographs of air bubbles in water. More recently, Jones (1965) carried out similar experiments, but his photographs are clearer and relatively larger than those of Haberman & Morton. The present theoretical shapes, figure 4, are several hundred times larger than the experimental shapes, which do not exceed the size of a dot in some cases.

It seems desirable, therefore, that more experiments should be done, with a view to obtaining enlarged and clearer photographs. Figure 5 shows the shapes

of argon bubbles in mercury but, to my knowledge, no such experimental results are yet available.

The bubble shapes in figures 4 and 5 are characterized by an indentation at the rear stagnation point. The size of the indentation increases with an increase in the Weber number. This effect is noted to be more pronounced in water than in mercury. In other words the rate of indentation growth, as the Weber number increases, is faster in high M liquids than in those with low M values.

8. Discussion

One of the objectives of this paper is to illustrate the potentialities of the virial method, in hydrodynamics, by applying it to the motion of gas bubbles. To some extent the method is a formal one since it presupposes a knowledge of the bubble shape, a thing which is usually lacking. However, it offers an efficient systematic way for the solution of certain problems where known methods may fail to do so. Earlier workers have demonstrated that the virial method, in some cases, leads to concrete results. Ledoux & Pekeris (1941), in their study of gaseous stars, using the virial method, obtained results which agree exactly with what follows from a strict variational treatment based on the same trial function. Chandrasekhar & Lebovitz (1963*a*, *b*) found that the linearized form of the virial equations permits exact and explicit solutions of problems associated with homogeneous masses.

In the present work, on expanding the expression (3.12) as $\chi \to 1$ (i.e. neglecting W^2), one finds

$$\chi = 1 + \tfrac{9}{64} W, \tag{8.1}$$

which agrees with Moore's (1959) linear theory. Thus the virial method gives the exact solution, of an oblate spheroid, if W^2 is negligible.

Let us now compare the virial result with that of Moore's (1965) approximate 'two-point theory'. First of all, the leading term in both results is identical with that in (8.1). Consider now figure 2, in which the 'two-point theory', the virial theory and their linearized versions are represented in terms of W versus χ. One finds that, for $\chi = 2$, the difference between these theories (curves A and C) is 1·4 %; for $\chi = 3$, 6·2 %; and for $\chi = 4$, 11·6 %. One may be tempted to say that the difference between them is an indication of the error involved in the spheroidal approximation. This may not be the case in view of the simplifying assumptions made in both theories. However, Moore (1965) has shown that his 'two-point theory' is reliable up to $\chi = 2$. This, at least, ensures that neither of these theories is far from the exact one, up to $\chi = 2$.

Further examination of figure 2 shows that there is a maximum Weber number of 3·271 at $\chi = 3{\cdot}72$ in the virial theory, as compared with 3·745 at $\chi = 6$ in the 'two-point theory'. Although the latter result is well outside the range of validity of the 'two-point theory' approximation, it is striking that the virial theory exhibits the same sort of behaviour, though at a smaller axis ratio of 3·72. This seems to support Moore's conjecture that "there is a maximum Weber number... above which the symmetric shape is impossible". It is

interesting to note that the maximum value attained by W in the virial theory differs only by about 2·8 % from the critical Weber number obtained by Hartunian & Sears (1957) for the onset of instability.

A remarkable feature of figure 2 is the way in which curves B and D, the curves that represent the linearized versions of the above theories, tend to converge towards each other. Although it is premature to conclude from this that the curve corresponding to the exact theory should lie in the intermediate region between these curves, it may be regarded as an indication that the exact curve is not far from this region.

I am grateful to Dr D. W. Moore of the Department of Mathematics, Imperial College, London, for much helpful discussion and criticism, and to the Sudan Government for a postgraduate scholarship.

Appendix

Here we give a special case of the method described by Weatherburn (1930, pp. 86–87) for the derivation of the first curvature of a surface. In order to avoid any ambiguities in the sign of the normal, we shall define $\mathbf{n}$ to be the unit normal to the surface directed away from the centre of curvature. Thus for an ellipsoidal surface, $\mathbf{n}$ denotes the unit outward normal. The first curvature J of the surface is then given by

$$J = \nabla . \mathbf{n}. \tag{A 1}$$

Consider now a family of surfaces

$$G(x, y, z) = \text{constant}, \tag{A 2}$$

where (x, y, z) are taken to be orthogonal curvilinear co-ordinates. This is a special case of the more general one, for the oblique co-ordinates, treated by Weatherburn. The unit normal $\mathbf{n}$ at any point on the surface G may then be expressed by

$$\mathbf{n} = F\nabla G, \tag{A 3}$$

where

$$F = 1/|\nabla G|. \tag{A 4}$$

Substituting from (A 3) into (A 1), the expression for the first curvature of the surface (A 2) becomes

$$J = F\nabla^2 G + \nabla F . \nabla G, \tag{A 5}$$

or

$$J = F\nabla^2 G + \mathbf{n} . \nabla \log G. \tag{A 6}$$

For our purpose, we shall take G to be a surface of revolution of the form

$$G = x - k - lg(y) = 0, \tag{A 7}$$

where k and l are constants and g is a single-valued continuous function of y.

REFERENCES

CHANDRASEKHAR, S. 1969 *Ellipsoidal Figures of Equilibrium*. Yale University Press.

CHANDRASEKHAR, S. & LEBOVITZ, N. R. 1963*a* *Astrophys. J.* **137**, 1142–1161.

CHANDRASEKHAR, S. & LEBOVITZ, N. R. 1963*b* *Astrophys. J.* **137**, 1162–1171.

EL SAWI, M. 1970 Ph.D. thesis, Imperial College, London.

FOX, L. 1957 *Numerical Solution of Two-point Boundary Problems*. Oxford University Press.

HABERMAN, W. L. & MORTON, R. K. 1953 An experimental investigation of the drag and shape of air bubbles rising in various liquids. *David Taylor Model Basin Rep.* no. 802.

HARPER, J. F., MOORE, D. W. & PEARSON, J. R. A. 1967 *J. Fluid Mech.* **27**, 361–366.

HARTUNIAN, R. A. & SEARS, W. R. 1957 *J. Fluid Mech.* **3**, 27–47.

JONES, D. R. M. 1965 Ph.D. dissertation, University of Cambridge.

LAMB, H. 1959 *Hydrodynamics*, 6th edn. Cambridge University Press.

LEDOUX, P. & PEKERIS, C. L. 1941 *Astrophys. J.* **94**, 124–135.

MOORE, D. W. 1959 *J. Fluid Mech.* **6**, 113–130.

MOORE, D. W. 1965 *J. Fluid Mech.* **23**, 749–766.

ROSENKILDE, C. E. 1967 *J. Math. Phys.* **8**, 84–88.

ROSENKILDE, C. E. 1969 *Proc. Roy. Soc.* A **312**, 473–494.

SAFFMAN, P. G. 1956 *J. Fluid Mech.* **1**, 249–275.

SHWERDTFEGER, K. 1968 *Chem. Engng Sci.* **23**, 937–938.

SIEMES, W. 1954 *Chem. Ing. Tech.* **26**, 614–630.

WEATHERBURN, C. E. 1930 *Differential Geometry of Three Dimensions*, vol. 2. Cambridge University Press.

WINNIKOW, S. & CHAO, B. T. 1966 *Phys. Fluids*, **9**, 50–61.